Korean J. Chem. Eng., 36(10), 1604-1618 (2019)
DOI: 10.1007/s11814-019-0345-4

pISSN: 0256-1115
eISSN: 1975-7220

Comprehensive potential evaluation of the bio-oil production and nutrient recycling from seven algae through hydrothermal liquefaction

Wenhan Song, Shuzhong Wang†, Donghai Xu, Yang Guo, Chuang Yang, Jiandong Zhang, and Yanhui Li

Key Laboratory of Thermo-Fluid Science & Engineering, Ministry of Education,
Xi'an Jiaotong University, Xi'an, Shaanxi 710049, China
(*Received 30 December 2018 • accepted 23 July 2019*)

Abstract−Hydrothermal liquefaction (HTL) of seven algae was conducted at both 280 and 350 °C with a reaction time of 30 min and a mass ratio of 1/4 of algae to water to evaluate the utilization potential of bio-oil production and nutrient recycling in the aqueous by-product and solid residue particles. *Chlorella* and *Nannochloropsis sp.* exhibited the highest bio-oil yields at 280 °C (36.5% from *Nannochloropsis* sp.) and 350 °C (38.1% from *Chlorella*). Additionally, temperature had little effect on the energy recovery from *Chlorella*, *Nannochloropsis* sp., *Spirulina*, *Cyanophyta* and *Euglena*. The carbohydrates and lipids in the algae were primarily related to monoaromatic and single-ring heterocyclic compound generation in bio-oil. In addition, carbohydrates and proteins significantly affected oxygenated compound production. The sizable total carbon, ammonia nitrogen, total nitrogen and phosphate contents in the aqueous by-products showed great potential as nutrient sources for algal cultivation and the production of value-added chemicals through recycling. Higher temperatures increased the percentage of ammonia nitrogen in the total nitrogen and reduced the phosphate concentration in the aqueous by-product. According to potential evaluation factors, *Chlorella*, *Nannochloropsis* sp., *Spirulina*, *Cyanophyta* and *Euglena* totally showed higher potential in terms of bio-oil production and aqueous nutrient recycling than *Dunaliella salina* and *Enteromorpha prolifera*, in which *Nannochloropsis* sp. exhibited the greatest utilization potential at investigated conditions.

Keywords: Hydrothermal Liquefaction, Bio-oil, Nutrient Recycling, Potential Evaluation, Algal Biomass Conversion

INTRODUCTION

Recent developments in the field of biomass conversion have led to renewed interest in bio-oil production. As an ideal biomass, algae are of great interest due to their fast growth, efficient photosynthesis, high lipid yield and reduced competition with food production for marginal lands [1]. Various conventional conversion routes, such as fast pyrolysis [2] and transesterification of lipids [3], can be utilized to produce bio-oil from algae. However, it is becoming extremely difficult to ignore the large amount of energy and time required for dewatering and drying. Hence, current methods are not suitable for high-moisture algae in particular. Hydrothermal liquefaction (HTL) is regarded as a promising approach for bio-oil production from wet algal biomass owing to its unique characteristics [4-6]. In the HTL process, water is in a subcritical liquid phase, enhancing the solubility of organic compounds and serving as a reactant and catalytic medium, so wet algal biomass can be directly converted to bio-oil while avoiding the energy penalty for drying [7,8]. In addition, HTL allows the conversion of not just lipids but also proteins and carbohydrates for bio-oil production [9,10]. Zhou et al. [11] conducted a preliminary study on the conversion of *Enteromorpha prolifera*, including lower fats to bio-oil by HTL. Song et al. [12] reported that a maximum yield of 31.79% was obtained from *Cyanophyta* (lipid content <5 wt%) harvested from Taihu Lake through the HTL process. Consequently, the reaction properties of HTL make it more applicable to the conversion of natural or whole algae in large-scale cultivation to bio-oil than in lab-scale in terms of economy and application potential [4].

Pioneering research on the hydrothermal liquefaction of algae was conducted by Dote et al. [13]. Subsequently, many investigators explored the influences of the reaction conditions on the yield and properties of bio-oil including using a wide range of reaction temperatures (220-375 °C) [14-16] and different algal strains [12] [17-23]. To date, it has been proven that temperature is the most influential reaction parameter on the chemical conversion process. Additionally, these previous studies with diverse algae strains were conducted in different reaction environments, such as reactors with various internal volumes, including 4.1 mL [20], 10 mL [24], 100 mL [25,26], 400 mL [19], 600 mL [27], 1 L [17,28], and 1.8 L [29], resulting in diverse bio-oil yields and properties from algae with small variations in biochemical composition. For example, Eboibi et al. [28] and Jena et al. [29] demonstrated different bio-oil yields (58 wt% in a 1 L reactor and 39.9 wt% in a 1.8 L reactor, respectively) from algae with similar biochemical compositions under similar reaction conditions. This inconsistency can be primarily attributed to variations in the heating rate or heat transfer rate in reactors of different volumes. Raheem et al. [30] found that the tar yield varied widely with changes in the heating rate (such as 12 wt% yield at 10 °C/min and 17 wt% at 20 °C/min, Table 3) under otherwise identical conditions. However, reactors with different volumes will

†To whom correspondence should be addressed.
E-mail: szwang@aliyun.com

necessarily have different heating rates due to variations in the heat transfer rates, resulting in different product distributions by HTL. Therefore, algae HTL performance in the consistent reaction environments needs to be further confirmed. Additionally, the aqueous phase (AP) after microalgae-HTL contains 4.6-43.9 wt% carbon, more than 50 wt% nitrogen and 28.3-100 wt% phosphorus relative to those constituents in the feedstock [14,15,31,32]. Chemical oxygen demand (COD) and the total organic carbon (TOC), total nitrogen (TN), ammonium and phosphorus contents in the AP were in the ranges of 60-100 g/L, 3-80 g/L, 0.77-31.7 g/L, 0.10-13.6 g/L, and 0.80-18.9 g/L, respectively [31,33,69]. These high levels of carbon, nitrogen and phosphorus in the post-HTL water complicated its safe disposal but provided a possible additional utilization for algae cultivation to decrease the feedstock cost [31,34], which dominated the total cost of fuel production [35]. Hence, Zhang et al. [36] proposed a novel system involving the synergistic integration of biocrude oil production via HTL with wastewater treatment through growing algae, referred to as environment-enhancing-energy (E^2-Energy). In addition, Selvaratnam et al. [37] presented a photosynthetically oxygenated waste-to-energy recovery (POWER) system to treat urban wastewater (UWW) for the highest net energy yield through a simulation approach. Generally, the TOC and nitrogen in the AP are more related to the proteins in the algae feedstock than the carbohydrates and lipids, and the nitrogen content is proportional to the reaction time [38-41]. The mass loading and metal content in the algae feedstock also significantly affect nitrogen and phosphorus in the AP [14,15,32,38,39,41]. Furthermore, the interactions between AP nutrient removal and algae or algae-bacterial growth in continuous HTL were also examined [42,43]. Although outstanding contributions to AP recycling have been reported, such studies primarily aimed to verify the characteristics of the post-HTL water, AP nutrient removal and growth of the algae or algae-bacteria consortium in the AP-containing medium. To the best of our knowledge, little research has been reported on the direct comparison and comprehensive potential assessment of different algae with the integration of bio-oil and AP characteristics under the same reaction conditions. Given this, it is difficult to make a reasonably comprehensive and systematic evaluation of the application potential of diverse algae through a HTL process. This information would be attractive for the development of whole algae-HTL processes for highly efficient energy and resource utilization.

To fill this knowledge gap, this work systematically advances the field by exploring the chemical compositions and properties of bio-oil, aqueous and residue products from seven algae as a function of two reaction temperatures (280 and 350 °C). In addition, a detailed characterization of the conversion paths and mechanism of the biochemical conversion of algal feedstock is provided. A comprehensive potential evaluation factor (ζ) was proposed to systematically estimate the application potential of algae HTL. This finding is expected to facilitate the establishment of a comprehensive evaluation system for algae HTL associated with subsequent nutrient recycling for algal cultivation.

EXPERIMENTAL SECTION

1. Materials

Spirulina (*Sp*) and *Chlorella* (*Ch*) powders were purchased from Wudi Lvqi Bioengineering Co., Ltd. *Enteromorpha prolifera* (*Ep*)

Table 1. Characteristics of algal feedstock (wt%)

	Ch	*Na*	*Sp*	*Cy*	*Eu*	*Du*	*Ep*
Proximate analysis*							
Moisture	2.2±0.1	5.3±0.1	4.9±0.1	3.6±0.2	3.0±0.1	4.0±0.0	2.3±0.2
Ash	5.6±0.3	6.4±0.1	4.9±0.2	4.4±0.3	5.7±0.2	0.6±0.1	2.6±0.3
Volatile matter	85.6±0.4	82.1±0.3	83.7±0.2	84.9±0.4	85.3±0.2	89.0±0.3	91.2±0.2
Fixed carbon	6.6±0.2	6.2±0.3	6.5±0.2	7.1±0.2	6.0±0.3	6.4±0.2	3.9±0.3
Elemental analysis							
C	48.7±1.3	42.1±1.1	45.5±1.3	50.1±1.0	41.3±1.6	42.9±1.2	29.9±1.5
H	7.5±0.6	6.5±0.5	7.0±0.6	7.6±0.8	6.4±0.5	6.9±0.4	6.0±0.8
N	11.6±2.1	8.3±1.4	9.3±1.9	9.0±1.6	9.4±2.0	0.6±0.2	3.8±0.8
S	2.4±0.2	1.5±0.2	3.3±0.4	2.2±0.3	0.9±0.2	0.5±0.1	6.7±0.5
O	29.8±1.9	41.6±1.0	34.9±1.4	31.1±1.2	42.0±1.5	49.1±0.6	53.6±1.1
H/C	1.9	1.9	1.9	1.8	1.9	1.9	2.4
O/C	0.5	0.7	0.6	0.5	0.8	0.9	1.3
N/C	0.2	0.2	0.2	0.2	0.2	<0.1	0.1
S/C	<0.1	<0.1	<0.1	<0.1	<0.1	<0.1	<0.1
HHV (MJ/kg)	22.1	16.2	19.5	22.4	15.7	15.6	9.7
Chemical composition analysis							
Protein	51.2±2.6	47.9±2.3	66±3.1	52.7±2.5	55.3±2.2	<0.1	21.1±1.3
Lipid	7.6±0.4	5.8±0.3	3.0±0.3	4.5±0.2	2.4±0.0	0.7±0.1	0.3±0.0
Carbohydrate	4.0±0.6	4.3±0.6	4.2±0.4	9.1±1.1	3.5±0.5	91.1±4.1	6.1±0.4

*As-receive basis

powder was provided by Jiangsu Qiangsheng International Trade Co., Ltd. *Nannochloropsis* sp. (*Na*) powder was obtained from Xi'an Jinheng Chemical Co., Ltd. *Dunaliella salina* (*Du*) and *Euglena* (*Eu*) powders were supplied by Shaanxi Sciphar Natural Products Co., Ltd. *Cyanophyta* (*Cy*) was collected from Taihu lake (moisture content >97%) in Wuxi China in August. Prior to HTL procedures, all algae samples were dried at 80 °C for >72 h, then ground and screened to powder (size <150 μm) for quantitative research. The fundamental characteristics of algae are shown in Table 1.

The solvents of anhydrous ether (purity: 99%), copper sulfate (purity: 99%), potassium sulfate (purity: 99%), sulfuric acid (purity: 97%), boric acid (purity: 99%), Bromoc-resol green indicator (purity: 99%), sodium hydroxide (purity: 99%), ethyl alcohol (purity: 95%) and dichloromethane (purity: 99%) were procured from Tianjin Hongyan chemical reagent factory. The chemicals of Methyl Red Indicator (purity: 99%), Methylene blue indicator (purity: 99%), hexane (purity: 97%), potassium iodide (purity: 99%) and ammonium chloride (purity: 99%) were supplied by Tianjin Fuchen chemical reagent factory. Potassium sodium tartrate (purity: 99%) was purchased from Tianjin Tianli chemical reagent factory. Mercury iodide (purity: 99%) was provided by Shanghai Shanpu chemical reagent factory.

2. Apparatus and Experimental Procedure

HTL experiments were performed in stainless steel mini-batch reactors (3.5 mL capacity) at two temperatures (280 and 350 °C) for 30 min with a mass ratio of 1/4 of algae to water at a water density of 0.59-0.77 g/mL. The calculated water densities at the corresponding reaction temperatures were determined utilizing water and steam properties calculating software (WASP). The required quantities of algal powder and deionized water were added into the reactors before the reactors were sealed. After preheating a Techne fluidized sand bath (SBS-4 type with a Techne TC-8D type temperature controller) to the reaction temperature, the reactors were placed into the sand bath and the reaction time started. The reactors reached the set temperature within approximately 2 min [44]. When the predetermined reaction time was reached, the reactors were removed and immersed in room-temperature water to quench the reaction.

After the reactions, each reactor was unscrewed and carefully rinsed into tubes using 9 mL of dichloromethane (DCM). The tubes were centrifuged (operating condition: 2,000 r/min for 20 min) to vertically stratify the reaction mixture into three layers (from top to bottom: the aqueous phase, the organic phase and the solid phase). The organic layer was transferred to a 15 mL vial, and the dichloromethane was removed for at least 12 h using a Termovap Sample Concentrator with nitrogen gas flowing at 45 °C through a gravimetric method. We measured the mass of the 15 mL vial (containing the bio-oil and DCM) every hour during the N_2 drying process. When the vial weight remained almost constant (accurate to one decimal place), we considered the DCM to have been completely removed. The material remaining in the vial was the algal bio-oil. Then, 5 mL of hexane was added, and the vial was shaken for several minutes to sufficiently separate the light components from the algal bio-oil (the hexane-soluble phase was light bio-oil, while the hexane-insoluble and dichloromethane-soluble phase was heavy bio-oil). The hexane was then removed from the light bio-oil at 75 °C using an approach similar to that used for dichloromethane evaporation. The aqueous by-products were retained for subsequent testing, and the remaining solid residue was dried for follow-up assessment. A schematic of the separation and recovery process for the algae HTL products is shown in Fig. 1. We conducted all experiments three times to ensure data repeatability.

3. Analysis Methods

The lipid, protein, and carbohydrate contents of the algae feedstock were measured through Soxhlet extraction method, the Kjeldahl method and anthrone colorimetry, respectively. The Soxhlet extraction method is shown below. First, a certain amount of algae was accurately weighed (accurate to three decimal places)

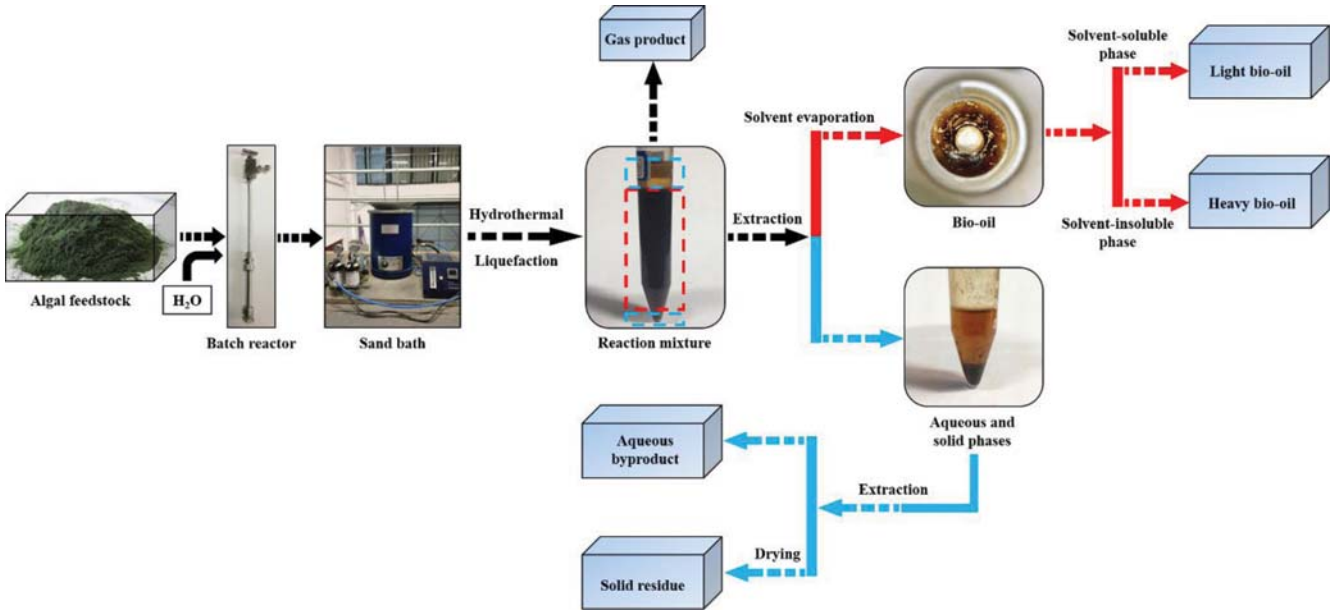

Fig. 1. The separation and recovery process schematic for algae HTL products.

and transferred to a filter paper cylinder. Second, the cylinder was placed into the extraction tube of the Soxhlet extractor. Third, petroleum ether was added to the extraction vessel and heated using a water bath until evaporation. Fourth, the heated petroleum ether was condensed by a condenser into the extraction tube to extract the lipids from the algal biomass (approximately 8 times per 1 h and holding for 6 h). When no oil spot was seen when dip testing the extracting solution using a ground glass rod, the extraction process was completed. Finally, the residual petroleum ether was dried for 1 h at 100±5 °C and cooled for 0.5 h, and the vessel containing the extract was weighed. Then, the drying, cooling and weighing process was repeated until a constant weight was reached (constant to one decimal place).

The Kjeldahl method was conducted as follows. First, a given mass of algae was accurately weighed (accurate to three decimal places) and transferred into a digestion tube. Second, 0.4 g of copper sulfate, 6 g of potassium sulfate and 20 mL of sulfuric acid were added to the algal sample in the digestion tube. Third, the digestor was heated to 420 °C and kept there for 1 h at which point the liquor in the digestion tube was green and transparent. After the digestion tube was removed, 50 mL of water was added to the tube, and the mixture was automatically distilled and titrated using an auto-Kjeldahl system (Foss Kjeltec 2300).

Anthrone colorimetry is commonly used to measure the carbohydrate content of plants, and the following procedure was used. First, glucose standards at different concentrations (0-80 μg/mL) were prepared in test tubes. Second, 4.0 mL of anthrone was immediately added into each test tube. Then, all the test tubes were tightly closed and immersed in a boiling water bath. After boiling for 10 min, the tubes were transferred to an ice bath to cool them to room temperature. A calibration curve was prepared from the glucose standard solutions using a visible spectrophotometer (BioTek Epoch, USA) at 620 nm. A specified volume of dried algae was weighed and transferred to a 50 mL triangular flask and 25 mL of boiling water added. The mixture was subjected to ultrasonic extraction for 10 min, and then the solution was filtered repeatedly into a 50 mL volumetric flask. Finally, a 1 mL aliquot of the solution diluted by a factor of 25 was analyzed following the procedure used to assess the glucose standard solutions. The soluble carbohydrate content was then determined from the calibration curve of glucose standard solutions.

The elemental composition (C, H, N and S) of the algal feedstock and bio-oil was determined by a Vario EL III elemental analyzer, and their standard deviations were less than 0.1%. The oxygen content was calculated by difference. Fourier transform infrared (FT-IR) spectroscopic analysis was performed on an FT-IR spectrometer (Germany Bruker Optics Vertex 70) to determine the functional groups in the bio-oil (scan range: 4,000-400 cm^{-1}, resolution=4 cm^{-1}). The microstructure and elemental composition of the solid residue were determined by scanning electron microscopy (SEM) (JEOL, model JSM-6390A) with energy dispersive spectrometry (EDS).

The key volatile oily compounds in the extracted bio-oil fraction were identified using a Shimadzu gas chromatograph-mass spectrometer (GCMS-QP2010 plus) equipped with a Restek Rtx-5 ms capillary column (30 m×0.25 mm i.d., 0.25 μm film thickness). All experiments were performed in electron ionization (EI, 70 eV) mode. The column temperature program was as follows: held at 60 °C for 1 min, then ramped to 170 °C at 5 °C/min and held for 1 min, then ramped to 300 °C at 3 °C/min and held for 8 min. This resulted in a total runtime of 76 min. The GC injector temperature was 300 °C, and the ion source temperature was 230 °C. The scanning range of the spectrometer was 30 to 500 m/z. Helium served as the carrier gas (1 mL/min). The injection volume was 0.4 μL for each sample, and the inlet split ratio was 20 : 1. Probability matching and the NIST08S mass spectral library were used to identify the compounds by confidence or similarity.

The total inorganic and organic carbon (TIC and TOC) content in the aqueous by-products was tested by a TOC analyzer (Shanghai EURO TECH, ET1020A). The furnace temperature was set at 680 °C. The sample ring volume was 33 μL, and the sampling time was 8 s. The ammonia nitrogen (NH_3-N) concentration in the aqueous phase was determined by a colorimetric method with Nessler's reagent and an ultraviolet-visible spectrophotometer (Shanghai Jinghua Instruments Co. Ltd., model: 752) with a test wavelength of 420 nm. The total nitrogen (TN) and phosphate (PO_4^-) concentrations were measured by a Spectroquant® NOVA60 water quality analyser by spectrophotometry. The pH value was measured to determine the acidity by universal and precise pH test papers.

4. Data Interpretation

In this study, the bio-oil yield, energy recovery, comprehensive potential evaluation factor (ζ) and potential evaluation factor (ζ_i) were defined as follows:

$$\text{Bio-oil yield (wt\%)} = \frac{\text{Mass of bio-oil}}{\text{Mass of algal feedstock}} \times 100\% \tag{1}$$

$$\text{Energy recovery (\%)} = \frac{\text{HHV of bio-oil} \times \text{mass of bio-oil}}{\text{HHV of feedstock} \times \text{mass of feedstock}} \times 100\% \tag{2}$$

$$\zeta = \sum_{n=1}^{5} \zeta_n \tag{3}$$

$$\zeta_1 = \frac{\text{Mass of bio-oil}}{\text{Mass of feedstock}} \tag{4}$$

$$\zeta_2 = \frac{\text{HHV of bio-oil}}{\text{HHV of feedstock}} \tag{5}$$

$$\zeta_3 = \frac{[\text{TIC}]}{[C^{algae}_{TIC(optimization)}]} \tag{6}$$

$$\zeta_4 = \frac{[NH_3\text{-N}]}{[C^{algae}_{NH_3\text{-}N(optimization)}]} \tag{7}$$

$$\zeta_5 = \frac{[\text{phosphate}]}{[C^{algae}_{phosphate(optimization)}]} \tag{8}$$

where [TIC], [NH_3-N] and [phosphate] represent the concentrations of these components in the aqueous by-products. Additionally, $[C^{algae}_{TIC(optimization)}]$, $[C^{algae}_{NH_3\text{-}N(optimization)}]$ and $[C^{algae}_{phosphate(optimization)}]$ are the required optimal concentrations of TIC, NH_3-N and phosphate in the algal culture solution, respectively, which are actual measured values and determined from previous research about algae cultivation.

The higher heating value (HHV) of the bio-oil derived from algae HTL was calculated with the Dulong formula [14]:

$$\text{Higher heating value (HHV, MJ/kg)} = 0.338C + 1.428(H - 0.125O) + 0.095S \quad (9)$$

where C, H, O and S represent the weight percentages of these elements in the material.

RESULTS AND DISCUSSION

1. Algal Feedstock Characterization

As shown in Table 1, all the algae feedstocks except *Enteromorpha prolifera* show similar H/C molar ratios of approximately 1.9. However, the algae samples have different C, N and S fractions. In particular, the highest C fraction was detected in *Cyanophyta* (50.1 wt%), and the other algae samples have content higher than 40 wt%, except for *Enteromorpha prolifera* (only 29.9 wt%). Compared with other lignocellulosic materials (nitrogen content <2 wt%), algae have higher levels of nitrogen, in the range of 0.6-11.6%, due to the protein content of the feedstock [10,19]. The sulfur content should not be ignored in view of sulfur oxide production, cylinder wear, deposit formation and contributions to particulate matter (PM) emissions in the burning process. All S/C values were lower than 0.1, showing that algae have a very low sulfur content, similar to that of lignocellulosic materials [10]. The high H/C atomic ratio of algae (1.8-2.4) indicates a high aliphatic content and the abundance of long chains with CH_2 groups [45]. As a highly important factor in energy utilization, algal HHV is immediately relevant to large-scale applications [46]. However, the HHVs of all the algae samples were lower than that of standard coal (29.3 MJ/kg) according to the Chinese National Standard (GB/T 2589-2008). Therefore, the direct application of algal biomass for fuel is inefficient. It is necessary to develop a novel method to convert algae into value-added fuels and chemicals with high efficiency.

The differences in the chemical compositions of various algal feedstocks are shown in Table 1. A maximum lipid content of 7.6 wt% and protein content of 66 wt% were derived from *Chlorella* and *Spirulina*, respectively. Additionally, *Dunaliella salina* had the highest carbohydrate content, with a value of 91.1 wt%. Generally, the typical chemical components of algae cells can be converted into the bio-oil fraction, and the contributions to the yield follow the trend lipids>proteins>carbohydrates, and these components contribute 80-55%, 18-11% and 15-6%, respectively [9,47].

2. Bio-oil Yields and Properties

2-1. Bio-oil Fraction and Solid Residue Production

Fig. 2 presents an overview of the light bio-oil, heavy bio-oil and solid residue yields derived from the HTL of seven algae at 280 and 350 °C, showing that bio-oil yields are different, which agrees with the characterization of the algal feedstocks. The bio-oil yields fluctuated in the range of 6.8-36.5 wt% at 280 °C and 18.1-38.1 wt% at 350 °C. This result indicates that higher temperatures promoted increased conversion of feedstocks and intermediates to bio-oils. At relatively low temperatures, the macromolecules in the feedstock (e.g., chlorophylls, celluloses and triglycerides) hydrolyze into water-soluble compounds and then generate high-molecular-weight compounds (e.g., aromatics, aliphatics, cycloalkanes and oxygenated hydrocarbons) through polymerization reactions [48]. Interestingly, harsh conditions can result in the conversion of certain heavy bio-oil fractions into light bio-oil fractions (e.g., phenols, naphthalenes, ketones, fatty acids, pyrroles, alcohols, benzenes, hydrocarbons, amides and amines), as free radicals can facilitate depolymerization [49,50]. The formation of gaseous products such as H_2, CO, CH_4, CO_2, C_2H_4, and C_2H_6 under the liquefaction conditions was negligible [14], and they were not detected in this investigation.

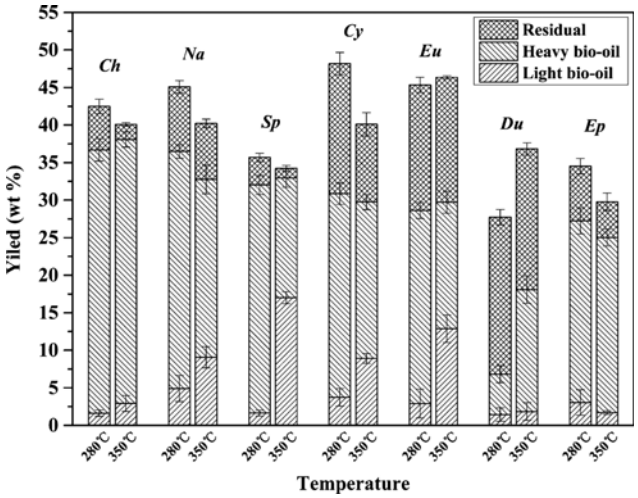

Fig. 2. Light bio-oil, heavy bio-oil and solid residue yields at 280 and 350 °C for 30 min of reaction time with a mass ratio of 1/4 of algae to water.

The two highest bio-oil yields of 38.1 wt% and 36.5 wt% were derived from *Chlorella* at 350 °C and *Nannochloropsis* sp. at 280 °C, respectively. After that, the bio-oil yields were in the narrow range of 28.6-33.0 wt% for *Spirulina*, *Cyanophyta* and *Euglena*. The two lower yielding materials were *Enteromorpha prolifera* and *Dunaliella salina*, and their yields varied in the range of 27.2-25.0 wt% and 6.8-18.1 wt%, respectively. Previous investigations [9,47] demonstrated that bio-oil was mainly generated from lipids and proteins. One possible conversion path in the HTL of lipids is the decomposition of lipids into various fatty acids, and these intermediates can form compounds such as alkanes, alkenes, and amides in the bio-oil fractions. The mechanism of bio-oil generation from proteins involves the hydrolysis of the peptide C-N bonds between the carboxyl and amine groups of amino acids, which are the building blocks of proteins. The amino acids formed by this process are subsequently degraded by decarboxylation and deamination [8].

The lowest bio-oil yields were both from *Dunaliella salina*, only approximately 6.8 wt% at 280 °C and 18.1 wt% at 350 °C, which was mainly due to its unique carbohydrate content (91.1 wt%), and this is consistent with similar algal cells, which have shown extremely low conversions into bio-oil [47]. In the HTL process, carbohydrates can be transformed into monosaccharides (such as glucose and fructose) by hydrolysis, and then into various substances such as furfurals, carboxylic acids, aldehydes and unstable intermediates [51], which tend to produce water-soluble compounds found in the aqueous by-product [19], possibly as a result of the large amounts of carbohydrates being degraded into polar water-soluble organics and not into non-polar hydrocarbon-type structures. Srokol et al. [51]

reported that the breakdown of glucose under similar hydrothermal conditions resulted in the formation of formic acid, acetic acid, lactic acid, acrylic acid, 2-furaldehyde and 1,2,4-benzenetriol. Most of these compounds are polar organic compounds that dissolve in the aqueous fraction and do not contribute to bio-oil formation.

The solid residue yield was below 10 wt% for the algae except *Dunaliella salina*, *Euglena* and *Cyanophyta*, and higher temperatures promoted decomposition, proving that almost all chemicals (>90 wt%) in the cells participated in the liquefaction reactions. However, the solid residue yields of these three algae were relatively higher (20.9-18.7 wt%, 16.7-16.6 wt% and 17.3-10.4 wt%, respectively), and this can be attributed to their higher production of water- and dichloromethane-insoluble components due to their high carbohydrate content. Chen et al. [52] proposed a potential HTL reaction route for carbohydrates. That is, hydrolysis of the carbohydrates to monosaccharides, and then these intermediates were further dehydrated to furfural derivatives. These compounds would then form cyclic oxygenated species through polymerization, and the final decomposition products could be distributed in the solid residue fraction. Moreover, the high ash and fixed-carbon content in the algal cells also contributed to the high residual yield due to the blanketing effect of the ash on the surface pores of the fixed carbon, which resulted in insufficient contact and reaction with subcritical water.

2-2. Bio-oil Properties

Table 2 shows the elemental compositions, HHVs and energy recoveries of the bio-oils derived from algae HTL at different temperatures with a reaction time of 30 min and a mass ratio of 1/4 of algae to water. The bio-oils from algae HTL had higher HHVs than those from algae feedstocks due to the higher carbon and hydrogen content and lower oxygen content of bio-oils, which is in agreement with previous HTL investigations of algae [12,20,24,26], lignocellulosic biomass [10], sludge [53] and swine manure [54]. This result reflects the potential future applicability of algae-based bio-oil as liquid fuel rather than the direct combustion of algae. High N/C and S/C ratios were observed compared with other feedstocks, such as lignocellulosic biomass [10] and sludge [53]. Therefore, it is necessary to remove the nitrogen and sulfur from the bio-oil in subsequent refining processes to lower the NO_x and SO_x emissions during combustion. The energy recovery represents the ratio of energy in the bio-oil fraction to that in the original algal feedstock. The highest value (68.1%) and lowest value (18.7%) of energy recovery were derived from *Enteromorpha prolifera* at 350 °C and *Dunaliella salina* at 280 °C, respectively. Furthermore, energy recovery changed from 3.1% to 12.8% for *Chlorella*, *Nannochloropsis* sp., *Spirulina*, *Cyanophyta* and *Euglena*, but varied greatly from 43% to 69% for *Dunaliella salina* and *Enteromorpha prolifera* with an increase in temperature. Therefore, the effect of temperature was not evident on the energy recovery for the former algae but was with the latter algae, primarily due to the nearly inverse trends in their bio-oil yields and HHVs at various temperatures.

2-3. Identification of the Key Volatile Oily Compounds in the Bio-oils

To elucidate the key volatile oily compounds in the bio-oil frac-

Table 2. Elemental compositions and HHVs of bio-oils derived from algae HTL at fixed 30 min with a mass ratio of 1/4 of algae to water

	Ch	*Na*	*Sp*	*Cy*	*Eu*	*Du*	*Ep*
Element & HHV (280 °C)							
C	73.4±2.2	64.0±1.7	68.1±2.3	64.8±1.5	67.4±2.0	74.5±1.9	59.0±1.3
H	8.5±0.3	8.0±0.1	8.6±0.3	7.7±0.6	9.0±0.2	6.4±0.3	5.9±0.5
N	6.7±0.2	6.3±0.1	7.1±0.2	7.0±0.3	8.0±0.2	0.2±0.0	5.4±0.3
S	0.7±0.1	0.7±0.0	0.8±0.0	0.7±0.0	0.9±0.1	0.5±0.0	1.6±0.1
O	10.7±1.3	21.0±1.5	15.4±2.0	19.8±0.8	14.7±1.7	18.4±1.4	28.1±0.9
H/C	1.4	1.5	1.5	1.4	1.6	1.0	1.2
O/C	0.1	0.2	0.2	0.2	0.2	0.2	0.4
N/C	0.1	0.1	0.1	0.1	0.1	<0.1	0.1
S/C	<0.1	<0.1	<0.1	<0.1	<0.1	<0.1	<0.1
HHV (MJ/kg)	35.1	29.4	32.6	29.4	33.1	31.1	23.5
Energy recovery (%)	58.1	63.8	50.6	40.3	57.9	18.7	47.6
Element & HHV (350 °C)							
C	73.5±1.8	67.0±1.4	72.6±2.2	79.1±2.0	72.5±1.9	74.8±1.6	71.5±2.1
H	8.4±0.4	6.7±0.1	8.8±0.1	8.9±0.2	8.4±0.3	6.8±0.2	8.7±0.4
N	6.5±0.1	5.6±0.2	6.7±0.2	0.7±0.0	7.3±0.2	0.2±0.0	5.9±0.2
S	0.6±0.1	1.5±0.1	0.7±0.1	0.7±0.0	1.2±0.1	0.3±0.0	0.6±0.1
O	11.0±1.3	19.2±0.7	11.2±1.6	10.6±1.9	10.6±1.3	17.9±1.3	13.3±1.0
H/C	1.4	1.2	1.5	1.4	1.4	1.1	1.5
O/C	0.1	0.2	0.1	0.1	0.1	0.2	0.1
N/C	0.1	0.1	0.1	<0.1	0.1	<0.1	0.1
S/C	<0.1	<0.1	<0.1	<0.1	<0.1	<0.1	<0.1
HHV (MJ/kg)	34.9	28.9	35.2	37.6	34.7	31.8	34.3
Energy recovery (%)	55.4	61.8	57.1	35.8	60.6	31.6	68.1

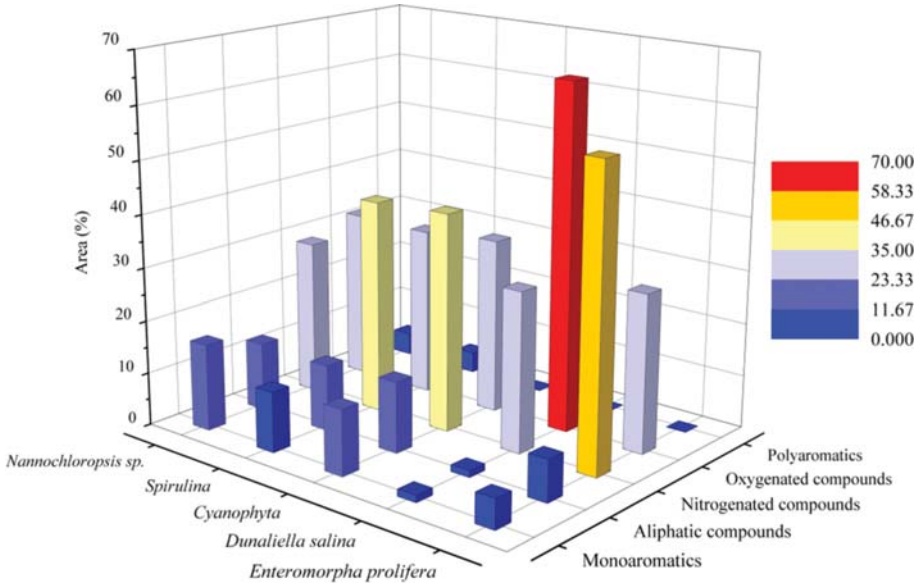

Fig. 3. Distribution of the key volatile oily compounds in bio-oils obtained from HTLs of five types of representative algae (reaction condition: 350 °C, 30 min, a mass ratio of 1/4 of algae to water).

tions, bio-oil samples obtained at 350 °C over 30 min at a mass ratio of 1/4 of algae to water from five typical and representative algae were characterized by GC-MS. The variations in the key volatile oily compounds in the bio-oils are summarized in Fig. 3. A total of 161 compounds were identified and are listed in the Supplementary Material. These compounds can be categorized into five types on the basis of their functional groups [15]: (1) monoaromatics and single-ring heterocyclic compounds such as benzene, phenol and their derivatives; (2) aliphatic compounds such as alkanes, alkenes, and their derivatives; (3) nitrogenated compounds such as amides, amines and nitrogen-containing heterocyclic compounds; (4) oxygenated compounds such as ketones, acids, esters and alcohols; and (5) polyaromatics such as fluorenes, anthracenes, naphthalene, benzoquinoline and their derivatives.

The differences in the peak areas of the compounds indicate the variations in the distribution of these key volatile oily compounds in the bio-oils from algae HTL. *Chlorella* and *Nannochloropsis* sp. exhibited the highest production of monoaromatics and single-ring heterocyclic compounds (16.4% from *Nannochloropsis* sp. HTL). As typical monoaromatics and single-ring heterocyclic compounds, phenols and their derivatives can generally be produced from the decomposition and conversion of the carbohydrates in algal cells, such as cellulose and glucose [55-57]. Luijkx et al. [58] proposed a potential reaction mechanism for the transformation of glucose into phenols in the HTL process. Carbohydrates are thought to be hydrolyzed into monosaccharides such as glucose or fructose and then converted into furan derivatives and finally phenols via rearrangement reactions associated with ring opening and closing. However, *Nannochloropsis* sp., which has a relatively low carbohydrate content, exhibited higher monoaromatic production. This might be attributable to the limitations of anthrone colorimetry, which was utilized for carbohydrate content determination in this study but can only be applied to the water-soluble fraction. *Nannochloropsis* sp. cells are covered by the thick cell wall made predominantly of the polysaccharide cellulose, and a small number of starch grains are present inside the cell [59]. These water-insoluble macromolecular substances might not be determined by this method.

The bio-oils of *Chlorella*, *Nannochloropsis* sp., *Spirulina*, *Cyanophyta* and *Euglena* had similar aliphatic content (12.6-13.4% of area), much higher than that from *Dunaliella salina* and *Enteromorpha prolifera* (<8% of area). This demonstrates that aliphatics were primarily derived from the lipids and proteins in algal cells. Under hydrothermal conditions, lipids were hydrolyzed into saturated and unsaturated fatty acids, which subsequently formed alkanes and alkenes by decarboxylation, respectively. Simultaneously, proteins were decomposed to amino acids and were then converted into organic acids by deamination [60] and ultimately converted to aliphatic compounds by decarboxylation; they may also be converted to aliphatic compounds first. Numerous alkanes were also observed in this investigation, consistent with previous algae research [9,29, 48,50,61]. In addition, heneicosane was found to be the major aliphatic compound in bio-oil, accounting for nearly half of the peak area of the aliphatic compounds. Interestingly, alkanes with chemical structures similar to heneicosane, such as eicosane and docosane, were also reported [9,50]. Moreover, a handful of cycloalkanes were generated from *Dunaliella salina* HTL, such as 1,2,3,4-tetramethylcyclobutane and 1-(phenylmethyl)-aziridine, in contents of 0.4% and 0.9%, respectively. In their investigation of *Laminaria saccharina* (also known as *Saccharina latissima*), Anastasakis and Ross also reported cycloalkanes in the bio-oil fraction [48].

Nitrogenated compounds in the bio-oils from *Spirulina* and *Cyanophyta* HTL accounted for approximately 40% of the material due to the similarities in the chemical compositions of these algae. The highest proportion of nitrogenated compounds in bio-oil was from *Enteromorpha prolifera* HTL, with a content of 56.4% despite its low nitrogen content (only 3.8%). The lowest value (29.2%) was obtained from *Nannochloropsis* sp. HTL although the nitrogen content in this algal was not the lowest. This is somewhat counter-

intuitive and surprising, and no statistically quantitative correlation between the content of nitrogenated compounds in the bio-oil and the nitrogen content in the algal feedstock was observed even though the nitrogen in bio-oil is widely considered to be derived from the proteins in the algae through hydrolysis and deamination [47,48,62]. The nitrogen-containing compounds in the bio-oil fraction could also be associated with the degree of dispersion of the nitrogen between the intermediates and final products, which is related to the characteristics of the algal cell structure and biochemical composition. Some investigators proposed that this distribution might be strongly influenced by the relative content of different fractions of algal [63,64].

During the conversion of proteins to other nitrogen-containing compounds, various reactions such as hydrolysis, deamination, aminolysis and cyclization may occur sequentially or simultaneously [52]. Therefore, nitrogen could be distributed into many types of compounds, such as amides, amines and heterocyclic compounds. Notably, the nitrogenated compounds from *Dunaliella salina* HTL mainly consisted of low-boiling and monocyclic compounds (all showed retention times of less than 20 min in the GC-MS results). This could be attributed to the generation of monosaccharides from the carbohydrates through hydrolysis and subsequent decomposition into low-carbon small molecules such as acids, ketones, and alcohols [52]. In contrast, the nitrogenated compounds from *Nannochloropsis* sp. HTL were mainly composed of high-boiling nitrogen-containing polycyclic compounds, such as indoles and pyrazines (all showed retention times greater than 20 min in the GC-MS results), which is related to the further decomposition of melanoidin, which was generated in the Maillard reaction of amino acids and small monosaccharides by dehydrogenation and cyclization reactions. In addition, long-chain high-boiling amides such as octadecanamide, N,N-dimethyloctanamide, and N-methyldodecanamide (all showed retention times of greater than 50 min in the GC-MS results) were found in the bio-oils produced from *Nannochloropsis* sp., *Spirulina*, *Cyanophyta*, *Enteromorpha prolifera* HTL. These amides were mainly produced from the conversion of proteins and lipids in the HTL process. The proteins were transformed into amino acids through hydrolysis, and these intermediates were converted to carbon dioxide, amines and alcohols via decarboxylation and to ammonia by deamination. Afterwards, the amines and ammonia could form amides in the presence of aminolysis. Additionally, amides could also originate from the decarboxylation of fatty acids, which are products of the hydrolysis of lipids.

The content of oxygenated compounds in the bio-oil fractions shows an apparent correlation with the carbohydrate and protein content in the algae, and the former factor is decisive. The highest content of oxygenated compounds was found in *Dunaliella salina*-derived bio-oil (approximately 65.2%) and those derived from the other algae had similar low content (29.7-33.0% of the total). In the HTL process, the carbohydrates were initially hydrolyzed into monosaccharides and acetic acid. Acetic acid is water-soluble and can be found in the aqueous fraction as a carbon source. Monosaccharides can be further decomposed into acids, ketones, alcohols, etc., or they can be transformed into furfural and its derivatives, which can form cyclic oxygenated species during polymerization. During cyclization and polymerization, the acids can also react with alcohols by esterification to form esters and their derivatives. However, cyclization and polymerization are favored over esterification. Therefore, the proportion of esters accounted for less than 50% of the oxygenated compounds generated from the other algae in the HTL. Due to the extremely low-protein and high-carbohydrate content, a great majority of the oxygenated compounds (97.6%) in the *Dunaliella salina*-derived bio-oil fraction were assigned as ketones and their derivatives.

Pioneering investigations [15,65,66] also proposed that polyaromatic species such as naphthalene and indene existed in the bio-oil fractions. However, only a few polyaromatic species were found from the *Spirulina* and *Nannochloropsis* sp. HTL, accounting for 3.9% and 4.3% of the total material, respectively, and the major compounds in this study were dibenzofuran and naphthalene derivatives.

In this investigation, FT-IR spectroscopy was utilized as an auxiliary and supplementary method to GC-MS analysis to estimate and compare the functional groups present in the bio-oils. The FT-IR spectra are illustrated in Fig. 4. The spectra of the bio-oils from the investigated algae HTL were similar, although certain individual variations appeared. The strongest absorption band of the bio-oils was near 3,430-3,286 cm^{-1}, and this band represents the O-H stretching vibration, showing the existence of compounds such as phenols and alcohols. Algae HTL-derived bio-oils contained benzene and aromatic compounds based on the absorption peak near 3,000 cm^{-1}, which represents the stretching vibrations of unsaturated =CH groups. Strong and sharp absorptions at 2,985-2,845 cm^{-1} (2,979 cm^{-1} and 2,856 cm^{-1}) represented symmetrical and asymmetrical C-H bonding stretching vibrations, suggesting the presence of aliphatic compounds. The high intensity of the narrow peak at 2,856 cm^{-1} in the bio-oil spectra can be attributed to hydroxyl groups. In addition, a strong absorbance at 1,668 cm^{-1} represented the stretching vibrations of C=C groups, which combined with the out-plane wagging vibration of the =CH groups of

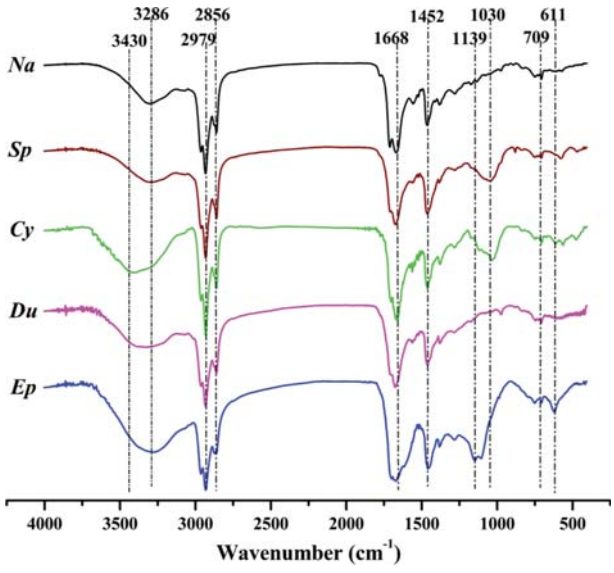

Fig. 4. FT-IR spectra of bio-oils obtained from HTLs of five types of representative algae (reaction condition: 350 °C, 30 min, a mass ratio of 1/4 of algae to water).

alkenes at 730-600 cm^{-1} (709 and 611 cm^{-1}), indicated the presence of alkenes and their derivatives. The absorbance peak at 1,452 cm^{-1} represents the scissoring of methylene groups, showing the existence of monocyclic aromatic compounds [9]. Significant differences appeared in the absorption peaks of 1,139 and 1,030 cm^{-1}, which are due to the appearance of amides and their derivatives. However, the bio-oils produced from *Spirulina*, *Cyanophyta* and *Euglena* HTL had strong absorption at 1,030 cm^{-1}, and a similar absorption band at 1,139 cm^{-1} was observed in the spectrum of the material from *Enteromorpha prolifera*, indicating the presence of various amides and their derivatives. Overall, the FT-IR spectra support the GC-MS analysis in this investigation.

3. Nutrient Analysis in the Aqueous By-product

The aqueous phase is a major by-product of algae HTL, and it contains a number of high-price nutrients and chemicals. Understanding the composition of the aqueous by-products is critical to further evaluating the overall potential of different algae HTL processes. Table 3 shows the primary nutrient concentrations such as the total inorganic carbon (TIC), total organic carbon (TOC), ammonium (NH_3-N), total nitrogen (TN), and phosphate content and the pH levels in the aqueous co-products after algae HTL.

The amount of TIC and TOC varied greatly, ranging from 0.01 to 53.8 g/L and 4.8 to 37.3 g/L, respectively. This indicates that a large proportion of the organic carbon in the algal feedstock was converted into water-soluble organic carbon compounds. Higher temperatures could promote the conversion of organic compounds into inorganic compounds. *Chlorella*, *Nannochloropsis* sp., *Spirulina*, *Cyanophyta* and *Euglena* had sizable total carbon content (TIC+ TOC) in their aqueous by-products. The inorganic carbon in the aqueous phase is involved in photosynthesis. Algae use the inorganic carbon as carbon source to convert light energy into chemical energy during photoautotrophic growth. Excessively high or low TIC concentration will lead to algae growth restriction [67]. As a consequence, the content of TIC is extremely important in the subsequent recycling of nutrients from algal cultivation. Although the TOC content reflected the recycling potential of high-price chemicals, such as aliphatic and aromatic species, the subsequent efficient extraction, separation and purification processes also need to be systematically and thoroughly studied. The highest [TIC] (53.8 g/L) was obtained from the HTL of *Spirulina*, and the highest [TOC] (37.3 g/L) was from *Dunaliella salina*, which could serve as a carbon source and source of value-added chemicals for recycling, respectively.

Nitrogen is essential for algae growth. In the cell, nitrogen is a vital participant in the synthesis of amino acids, purines, pyrimidines, amines and chlorophyll during photosynthesis. Algal cell growth would be restrained with weakened cellular photosynthesis if insufficient nitrogen was present. Conversely, excess nitrogen would also suppress algal growth, and this could arise due to an imbalance of nitrogen and phosphorus [68]. Among available nitrogen sources, only NH_3-N can be directly absorbed and utilized to synthetize amino acids, whereas other nitrogen sources must be transformed into NH_3-N prior to participating in algal cell metabolism [69]. The NH_3-N and TN concentrations in the aqueous phase fluctuated from 0.4 to 18.1 g/L and from 1.1 to 22.0 g/L, respectively. In general, the variations in NH_3-N and TN were well correlated in different algae. *Spirulina*, *Cyanophyta* and *Euglena* showed higher concentrations of NH_3-N and TN in their aqueous by-product due to their high content of nitrogen-containing compounds, such as protein and chlorophyll [62]. Moreover, there were no rigid trends in [NH_3-N] and [TN] with increasing temperature, whereas temperature increased the proportions of NH_3-N in TN, which

Table 3. Nutrients and pH measurements in the aqueous product after HTL

	Ch	*Na*	*Sp*	*Cy*	*Eu*	*Du*	*Ep*
Carbon, nitrogen, phosphorus resources and pH (280 °C, 30 min, a mass ratio of 1/4 of algae to water)							
Concentration (g/L)							
[TIC][a]	36.2±0.9	36.4±1.1	45.4±1.0	38.1±1.0	35.2±0.8	0.01±0.0	0.8±0.0
[TOC][b]	22.3±1.0	25.0±0.8	14.6±0.9	11.4±0.6	18.2±0.7	37.3±1.1	34.1±0.6
[NH_3-N]	6.0±0.0	8.4±0.0	10.6±0.1	3.8±0.0	7.5±0.0	0.4±0.0	1.5±0.0
[TN]	17.2±0.1	10.0±0.0	20.0±0.2	15.0±0.1	14.5±0.0	2.4±0.0	5.9±0.0
NH_3-N/TN (%)	34.9	84.1	53.0	25.1	51.7	27.1	24.6
Phosphate	1.3±0.0	0.7±0.0	1.6±0.0	0.2±0.0	0.5±0.0	0.9±0.0	0.2±0.0
pH	7.2±0.2	8.5±0.3	8.5±0.2	8.5±0.3	8.2±0.3	2.5±0.2	6.0±0.3
Carbon, nitrogen, phosphorus resources and pH (350 °C, 30 min, a mass ratio of 1/4 of algae to water)							
Concentration (g/L)							
[TIC][a]	41.3±1.0	48.2±0.9	53.8±1.2	46.8±1.3	48.5±0.9	0.1±0.0	7.9±0.3
[TOC][b]	17.5±0.6	9.9±0.5	4.8±0.2	14.5±0.4	7.8±0.4	28.3±1.0	23.9±0.8
[NH_3-N]	10.2±0.2	12.8±0.3	18.1±0.1	10.2±0.2	10.2±0.2	0.7±0.0	2.7±0.0
[TN]	16.0±0.2	14.6±0.1	22.0±0.1	17.2±0.1	16.5±0.2	1.1±0.0	4.5±0.0
NH_3-N/TN (%)	63.8	87.5	82.4	59.3	61.6	34.6	60.4
Phosphate	1.3±0.0	0.4±0.0	1.2±0.0	0.2±0.0	0.3±0.0	0.1±0.0	0.1±0.0
pH	8.5±0.3	9.0±0.2	8.8±0.2	9.0±0.2	8.5±0.3	3.0±0.2	7.0±0.2

[a]Total inorganic carbon

[b]Total organic carbon

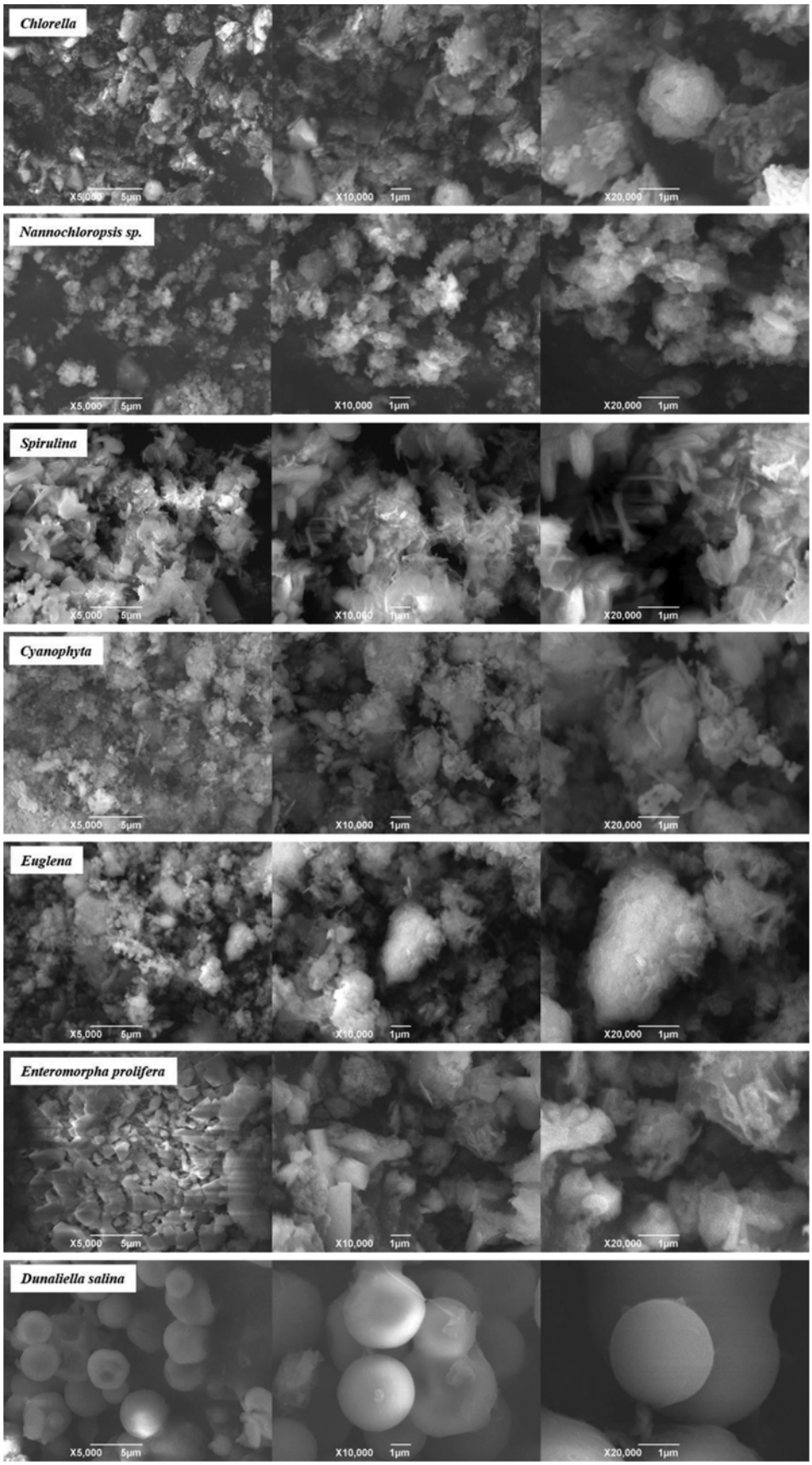

Fig. 5. SEM images of solid residue particles from seven algae HTLs under the condition of 350 °C, 30 min and a mass ratio of 1/4 of algae to water.

was similar to previous research [14,70]. In view of the high [NH_3-N], the aqueous by-products of all the algae except *Dunaliella salina* and *Enteromorpha prolifera* were alkaline (pH=7.0-9.0). The aqueous products of *Dunaliella salina* and *Enteromorpha prolifera* were acidic (pH<7.0). Maddi et al. [71] reported that the aqueous by-products from algae with high lipid and low nitrogen content tended to be acidic. The pH increased slightly as the temperature increased, probably due to the higher proportion of NH_3-N in the TN. A high [NH_3-N] in the aqueous by-products indicated a great potential for nitrogen recycling for algal cultivation and the production of high-price chemicals.

As a primary nutrient for algae growth, phosphorus plays a key role in the synthesis of carbohydrates, proteins and lipids. However, algae chiefly absorb inorganic phosphorus rather than organic phosphorus. The absorbed exogenous inorganic phosphorus is transported into the algae cells as soluble phosphates. A majority of these phosphate species exists in the cytoplasm, and others are converted to polyphosphates for energy storage and applied in the synthesis of other cell components, such as phospholipids [72]. Compared with carbon and nitrogen sources, phosphate is much less abundant in the aqueous by-products, and the concentrations varied from 0.1 to 1.6 g/L due to the low levels of phosphorous-containing compounds such as phospholipids, nucleic acids, and adenosine triphosphate (ATP) in algal cells. Additionally, it also tends to decrease with increasing temperature for all algae, which is similar to what was found in a prior study [73]. This trend was consistent with the higher content of phosphate observed in the solid residues obtained at higher temperatures.

4. Nutrient Analysis in the Solid Residue

4-1. Surface and Bulk Structure Analysis of the Solid Residue

Fig. 5 depicts that solid residue particles had various surfaces and bulk structures. The characteristics of the solid residue, such as particle size, aggregation and adhesion, are relevant to subsequent processing steps. For example, larger or adhered particles are likely to plug processing systems. Therefore, the characterization of the solid residue particles is significant for industrial applications. The solid residue particles were clearly agglomerated and adhered, except for those of *Dunaliella salina* and *Enteromorpha prolifera* HTL. Garcia Alba and co-workers [74] presented a possible explanation for this clustering and adhesion; it could be the result of precipitation or coagulation due to thermal denaturation of the proteins in the algal cells. Furthermore, the adhesion of the solid residue particles can be related to the viscous gels generated during the heating process [75]. Additionally, the Maillard reaction can promote clustering due to melanoidin or polymer formation [76], which was more significant for *Cyanophyta*. Moreover, aggregation can be due to

Table 4. Elemental composition of the solid residue collected after HTL (reaction conditions: 280 and 350 °C, 30 min, a mass ratio of 1/4 of algae to water)

	Ch	*Na*	*Sp*	*Cy*	*Eu*	*Du*	*Ep*
Element (280 °C) (wt%)							
C	58.6±2.4	32.1±1.5	45.8±1.5	24.5±1.4	32.7±1.3	82.0±1.9	48.3±1.9
O	25.9±1.3	29.7±1.2	31.0±1.3	32.7±1.3	26.5±1.1	15.8±0.6	26.1±1.2
Na	0.6±0.0	2.2±0.1	0.8±0.0	0.3±0.0	1.2±0.1	<0.01	1.3±0.0
Mg	2.2±0.1	7.0±0.3	4.0±0.1	2.3±0.0	3.3±0.2	<0.01	4.6±0.4
Al	0.4±0.0	1.3±0.1	0.7±0.1	2.8±0.1	3.5±0.2	0.01±0.0	0.5±0.0
Si	0.4±0.0	2.9±0.1	0.6±0.0	6.9±0.4	6.7±0.2	<0.01	1.4±0.1
P	5.4±0.3	10.7±0.4	9.4±0.4	8.2±0.2	9.3±0.3	0.1±0.0	4.1±0.1
S	0.9±0.1	0.6±0.0	0.4±0.0	0.7±0.0	0.6±0.0	0.5±0.0	5.0±0.2
Cl	0.3±0.0	3±0.1	0.4±0.0	0.04±0.0	0.4±0.0	0.4±0.0	2.7±0.0
K	1.3±0.1	1.2±0.0	4.3±0.2	1.2±0.0	3.1±0.1	<0.01	2.7±0.1
Ca	3.3±0.1	7.6±0.2	1.9±0.0	18.2±1.0	8.8±0.3	0.5±0.0	2.4±0.0
Fe	0.8±0.0	1.7±0.0	0.9±0.1	2.4±0.1	4.0±0.1	0.7±0.0	1.1±0.1
Element (350 °C) (wt%)							
C	48.9±2.5	23.9±1.1	36.8±1.4	22.2±0.9	22.5±0.8	76.5±1.8	27.7±1.1
O	28.6±1.2	31.5±1.3	31.3±1.2	32.8±1.6	34.7±1.8	21.9±0.9	36.7±1.7
Na	0.7±0.0	4.2±0.1	2.2±0.1	0.4±0.0	0.6±0.0	0.2±0.0	1.0±0.1
Mg	3.8±0.2	7.8±0.2	6.9±0.3	3.0±0.1	4.0±0.2	0.1±0.0	9.2±0.5
Al	0.4±0.0	1.2±0.0	0.9±0.0	3.2±0.1	4.0±0.2	0.1±0.0	0.3±0.0
Si	0.6±0.0	2.2±0.1	1.4±0.0	7.5±0.2	8.0±0.1	<0.01	0.8±0.0
P	8.9±0.4	12.0±0.4	12.2±0.3	9.1±0.2	9.9±0.2	<0.01	12.4±0.5
S	0.4±0.0	0.8±0.0	0.4±0.0	0.7±0.0	0.3±0.0	0.2±0.0	4.8±0.2
Cl	0.1±0.0	4.5±0.1	0.2±0.0	0.1±0.0	0.1±0.0	0.6±0.0	1.5±0.1
K	1.7±0.1	1.8±0.1	3.9±0.2	1.7±0.0	1.8±0.1	0.4±0.0	2.1±0.1
Ca	5.3±0.1	8.3±0.2	2.8±0.1	16.9±0.7	9.6±0.2	0.02±0.0	3.2±0.1
Fe	0.7±0.0	1.7±0.1	1.1±0.0	2.4±0.1	4.7±0.2	0.1±0.0	0.4±0.0

the low dielectric constant of the subcritical water surrounding the algal cells [74]. For *Dunaliella salina* and *Enteromorpha prolifera*, the particles are more likely to accumulate than adhere based on the visible distinct interparticle boundaries. What is striking is that the solid residue from *Dunaliella salina* HTL appeared to be regularly spherical, which is mainly attributed to the relatively high non-differentiation and homogeneity of the chemical composition of the algal cells (carbohydrates account for 91.1 wt% of the total chemical components). Additionally, in those reaction conditions, the water provided an approximately homogenous reaction as a result of the extremely high solubility [7].

4-2. Elemental Composition Analysis of the Solid Residue

Table 4 shows the elemental composition of the solid residue after HTL for 30 min at a mass ratio of 1/4 of algae to water. These data reveal that the solid residues mainly contained C and O (accounting for >70 wt% of the total mass fraction) and other primary nutrient elements (such as Mg, P, Ca, and K) contributed 12.2 wt% and 19.7 wt% at 280 °C and 350 °C, respectively. Their presence is probably due to bioaccumulation in algae during the growth process. Anastasakis et al. [48] demonstrated that most of the potassium and sodium were distributed in the aqueous fraction, while the majority of the calcium and magnesium was in the solid phase. In our research, Mg and P were also largely found in the solid residue, and Mg and P are essential nutrients for photosynthesis in the algal growth process. In addition, a higher temperature favored the transfer of most nutrient elements to the solid residue, making it a high-price nutrient source.

5. Comprehensive Potential Evaluation of Bio-oil Production and Nutrient Recycling for Algal Cultivation in the Aqueous By-product

In this investigation, the potential evaluation factor ζ_i was proposed to evaluate the applicative potential of the main products, including the bio-oil and aqueous nutrients (e.g., C, N, and P). $[C^{algae}_{TIC(optimization)}]$, $[C^{algae}_{NH_3\text{-}N(optimization)}]$ and $[C^{algae}_{phosphate(optimization)}]$ were derived from corresponding research, as shown in Table 5. Higher ζ_1 and ζ_2 values indicate higher bio-oil yields and bio-oil HHVs, respectively, and correspond to greater potential for bio-oil production. The values of ζ_3, ζ_4 and ζ_5 represent the ratios of nutrients in the post-HTL water relative to the required optimal nutrient concentrations of the corresponding algal, showing higher allowable dilution multiples for optimally culturing algae. Larger values of ζ_3, ζ_4 and ζ_5 correspond to greater potentials for culturing algae

Table 5. Required optimal concentrations of TIC, NH_3-N and phosphate in algal culture solution

Algae	$[C^{algae}_{TIC(optimization)}]$ (g/L)	$C^{algae}_{NH_3\text{-}N(optimization)}]$ (g/L)	$[C^{algae}_{phosphate(optimization)}]$ (g/L)	References
Ch	0.143	0.084	0.014	[77]
Na	0.120	0.017	0.004	[78]
Sp	7.143	0.401	0.436	[79]
Cy	0.083	0.301	0.017	[80]
Eu	0.060	0.327	0.600	[81]
Du	0.714	0.101	0.042	[82]
Ep	0.210	0.018	0.004	[83]

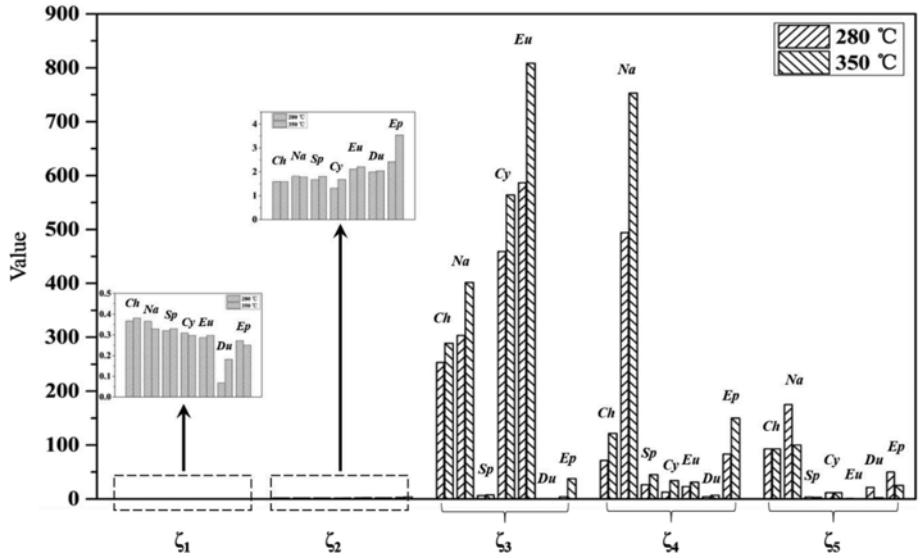

Fig. 6. Potential evaluation factor ζ_i of bio-oil and aqueous products from algae HTL at investigated conditions (ζ_1 represents the ratio of the bio-oil mass to the feedstock mass; ζ_2 represents the ratio of the bio-oil HHV to the feedstock HHV; ζ_3 represents the ratio of the TIC concentration to the required optimal TIC concentration; ζ_4 represents the ratio of the NH_3-N concentration to the required optimal NH_3-N concentration; ζ_5 represents the ratio of the phosphate concentration to the required optimal phosphate concentration.).

Table 6. Comprehensive potential evaluation factor ζ of bio-oil production and aqueous nutrients for algae cultivation after HTL (reaction conditions: 280 and 350 °C, 30 min, a mass ratio of 1/4 of algae to water)

Temperature	*Ch*	*Na*	*Sp*	*Cy*	*Eu*	*Du*	*Ep*
280 °C	419.4	974.6	38.5	485.0	612.8	27.5	139.8
350 °C	505.1	1256.7	57.6	611.5	842.5	11.7	216.4

by the post-HTL water. All the ζ_i values of the seven algae are shown in Fig. 6. The resultant comprehensive potential evaluation factor, ζ, is shown in Table 6.

Fig. 6 shows various potential evaluation factor values (ζ_1, ζ_2, ζ_3, ζ_4, and ζ_5) of the algae-based bio-oils and aqueous products obtained at 280 and 350 °C for 30 min at a mass ratio of 1/4 of algae to water. *Dunaliella salina* and *Enteromorpha prolifera* exhibited smaller values of ζ_1 than *Chlorella*, *Nannochloropsis* sp., *Spirulina*, *Cyanophyta* and *Euglena*, corresponding to lower bio-oil yields. All values of ζ_2 were greater than 1, proving that the HHVs of the bio-oils were higher than those of the feedstock and that higher temperatures would improve ζ_2 by increasing the HHV of the bio-oil. The highest value of ζ_3 was obtained from *Euglena* HTL, and much lower ζ_3 values were obtained from *Spirulina*, *Dunaliella salina* and *Enteromorpha prolifera*, which was mainly due to higher required TIC concentrations for its optimal cultivation relative to other algae. *Nannochloropsis* sp. showed the highest ζ_4 value as it requires the lowest NH_3-N concentration. More water would be consumed during dilution to avoid the excess NH_3-N inhibiting the growth of the algal cells [69]. *Chlorella* and *Nannochloropsis* sp. showed relatively higher ζ_5 values as their required phosphate concentrations were lower.

Table 6 reveals the comprehensive potential evaluation factors, ζ values, for the bio-oil and aqueous material produced by algae HTL. *Chlorella*, *Nannochloropsis* sp., *Spirulina, Cyanophyta* and *Euglena* exhibited higher ζ values than *Dunaliella salina* and *Enteromorpha prolifera* and generally showed much greater utilization potential from algal HTL. However, the ζ value of *Spirulina* was lower than that of *Enteromorpha prolifera* due to the higher required nutrient concentration for the culture solution. Notably, *Nannochloropsis* sp. had the highest ζ value, showing the greatest application potential regardless of temperature.

CONCLUSIONS

We systematically evaluated the potential of bio-oil production and high-price nutrient recycling of the aqueous by-products and solid residue after batch HTL of seven algae. *Chlorella* and *Nannochloropsis* sp. exhibited the highest bio-oil yield at 280 °C (36.5 wt% from *Nannochloropsis* sp.) and 350 °C (38.1 wt% from *Chlorella*). Higher temperatures generally promoted sufficient bio-oil production, especially for the transformation of the heavy bio-oil fraction into the light fraction. The maximum energy recovery (68.1%) was obtained from *Enteromorpha prolifera* at 350 °C for 30 min at a mass ratio of 1/4 of algal to water. Temperature had little effect on the energy recovery for *Chlorella*, *Nannochloropsis* sp., *Spirulina*, *Cyanophyta* and *Euglena*.

The GC-MS and FT-IR analysis results confirmed that *Chlorella* and *Nannochloropsis* sp. had the highest content (16.4% from *Nannochloropsis* sp.) of monoaromatics and single-ring heterocyclic compounds. *Chlorella*, *Nannochloropsis* sp., *Spirulina*, *Cyanophyta* and *Euglena* algae had higher aliphatic contents (12.6-13.4% of area) than *Dunaliella salina* and *Enteromorpha prolifera* (<8% of area), indicating that the aliphatic species were mostly derived from lipids and proteins. No strict quantitative relationship between the contents of nitrogenated compounds in the bio-oil and the nitrogen in the algae was observed. The content of oxygenated compounds in the bio-oil fractions was affected by the content of carbohydrates and proteins in the algae, especially for the carbohydrate content.

The aqueous by-products of *Chlorella*, *Nannochloropsis* sp., *Spirulina*, *Cyanophyta* and *Euglena* had high total carbon content (TIC+TOC). The highest [TIC] (53.8 g/L) was obtained from *Spirulina*, and the highest [TOC] (37.3 g/L) was from *Dunaliella salina*, indicating that they could serve as a sufficient carbon source for algal cultivation and as platform for the production of value-added chemicals through recycling, respectively. The concentrations of ammonia nitrogen (NH_3-N) and total nitrogen (TN) in the aqueous phases ranged from 0.4 to 18.1 g/L and from 1.1 to 22.0 g/L, respectively, indicating that it has great potential as the nitrogen source for algal cultivation and is valuable for nitrogenous chemical recycling. The aqueous by-products of *Spirulina*, *Cyanophyta* and *Euglena* showed higher concentrations of NH_3-N and TN. No rigid trends in the NH_3-N and TN concentrations were found with increasing temperature, whereas temperature could increase the proportion of NH_3-N in the TN. The phosphate concentration in the aqueous phase varied from 0.1 to 1.6 g/L and showed a downtrend as the temperature increased. The aqueous by-products from *Chlorella*, *Nannochloropsis* sp., *Spirulina*, *Cyanophyta* and *Euglena* HTL were alkaline (pH=7.0-9.0), whereas those from *Dunaliella salina* and *Enteromorpha prolifera* HTL were acidic (pH<7.0).

The solid residue particles from *Chlorella*, *Nannochloropsis* sp., *Spirulina*, *Cyanophyta* and *Euglena* HTL tended to cluster and adhere to each other, whereas those from *Dunaliella salina* and *Enteromorpha prolifera* were more likely to exhibit accumulation with apparent edges among the particles. The solid residue also contained many nutrient elements, such as P and K, giving it great potential as a resource for subsequent algal cultivation, and higher temperatures would facilitate the transfer of these elements into the solid residue.

In conclusion, *Chlorella*, *Nannochloropsis* sp., *Spirulina*, *Cyanophyta* and *Euglena* generally had higher ζ values than *Dunaliella salina* and *Enteromorpha prolifera*, and higher temperatures could improve ζ. The highest ζ values were from *Nannochloropsis* sp. HTL, which indicated it possessed the greatest potential applicability of all the algae investigated in this research at both 280 and 350 °C for 30 min at a mass ratio of 1/4 of algae to water.

ACKNOWLEDGEMENT

This research is supported by Fundamental Research Funds for the Central Universities [xjj2018006], National Natural Science Foundation of China (Grant No. 51876174 and 21576219) and Shaanxi Province Natural Science Foundation of China (2018JM5011).

SUPPORTING INFORMATION

Additional information as noted in the text. This information is available via the Internet at http://www.springer.com/chemistry/journal/11814.

REFERENCES

1. P. Schenk, S. Thomas-Hall, E. Stephens, U. Marx, J. Mussgnug, C. Posten, O. Kruse and B. Hankamer, *Bioenerg Res.*, **1**(1), 20 (2008).
2. X. Miao, Q. Wu and C. Yang, *J. Anal. Appl. Pyrolysis*, **71**(2), 855 (2004).
3. H. Xu, X. Miao and Q. Wu, *J. Biotechnol.*, **126**(4), 499 (2006).
4. P. E. Savage, *Science*, **338**(6110), 1039 (2012).
5. D. López Barreiro, W. Prins, F. Ronsse and W. Brilman, *Biomass Bioenergy*, **53**, 113 (2013).
6. C. Tian, B. Li, Z. Liu, Y. Zhang and H. Lu, *Renew. Sust. Energy Rev.*, **38**, 933 (2014).
7. N. Akiya and P. E. Savage, *Chem. Rev.*, **102**(8), 272 (2002).
8. A. A. Peterson, F. Vogel, R. P. Lachance, M. Froling, J. M. J. Antal and J. W. Tester, *Energy Environ. Sci.*, **1**(1), 32 (2008).
9. P. Duan and P. E. Savage, *Ind. Eng. Chem. Res.*, **50**(1), 52 (2010).
10. L. Cao, G. Luo, S. Zhang and J. Chen, *RSC Adv.*, **6**(18), 15260 (2016).
11. D. Zhou, L. Zhang, S. Zhang, H. Fu and J. Chen, *Energy Fuel*, **24**(7), 4054 (2010).
12. W. H. Song, S. Z. Wang, Y. Guo and D. H. Xu, *Int. J. Hydrogen Energy*, **42**(31), 20361 (2017).
13. Y. Dote, S. Sawayama, S. Inoue, T. Minowa and S.-y. Yokoyama, *Fuel*, **73**(12), 1855 (1994).
14. P. J. Valdez, M. C. Nelson, H. Y. Wang, X. N. Lin and P. E. Savage, *Biomass Bioenergy*, **46**, 317 (2012).
15. U. Jena, K. C. Das and J. R. Kastner, *Bioresour. Technol.*, **102**(10), 6221 (2011).
16. T. M. Brown, P. G. Duan and P. E. Savage, *Energy Fuel*, **24**(6), 3639 (2010).
17. C. Miao, M. Chakraborty and S. Chen, *Bioresour. Technol.*, **110**, 617 (2012).
18. P. J. Valdez and P. E. Savage, *Algal Res.*, **2**(4), 416 (2013).
19. S. S. Toor, H. Reddy, S. Deng, J. Hoffmann, D. Spangsmark, L. B. Madsen, J. B. Holm-Nielsen and L. A. Rosendahl, *Bioresour. Technol.*, **131**, 413 (2013).
20. Y. Guo, W. H. Song, J. M. Lu, O. R. Ma, D. H. Xu and S. Z. Wang, *Algal Res.*, **11**, 242 (2015).
21. B. Zhang, Q. S. Lin, Q. H. Zhang, K. J. Wu, W. H. Pu, M. D. Yang and Y. L. Wu, *RSC Adv.*, **7**(15), 8944 (2017).
22. C. Yang, L. Jia, C. Chen, G. Liu and W. Fang, *Bioresour. Technol.*, **102**(6), 4580 (2011).
23. W. Yang, X. Li, S. Liu and L. Feng, *Energy Convers. Manage.*, **87**, 938 (2014).
24. L. B. Diego, S. Chiara, T. Giuseppe, H. Ursel, K. Andrea and P. Wolter, *Bioresour. Technol.*, **174**, 256 (2014).
25. S. P. Zou, Y. L. Wu, M. D. Yang, C. Li and J. M. Tong, *Energy Environ. Sci.*, **3**(8), 1073 (2010).
26. J. W. Lu, Z. D. Liu, Y. H. Zhang, B. M. Li, Q. Lu, Y. Q. Ma, R. X. Shen and Z. B. Zhu, *J. Clean Prod.*, **142**, 749 (2017).
27. C. Hognon, F. Delrue, J. Texier, M. Grateau, S. Thiery, H. Miller and A. Roubaud, *Biomass Bioenergy*, **73**, 23 (2015).
28. B. E.-O. Eboibi, D. M. Lewis, P. J. Ashman and S. Chinnasamy, *Bioresour. Technol.*, **174**, 212 (2014).
29. U. Jena, K. C. Das and J. R. Kastner, *Appl. Energy*, **98**, 368 (2012).
30. R. Abdul, W. A. K. G. Wan Azlina, Y. H. Taufiq Yap, M. K. Danquah and H. Razif, *RSC Adv.*, **5**(88), 71805 (2015).
31. L. J. Leng, J. Li, Z. Y. Wen and W. G. Zhou, *Bioresour. Technol.*, **256**, 529 (2018).
32. B. V. Mariluz, S. S. Ulrike, P. Gael, V. Frederic and L. Christian, *Algal Res.*, **8**, 76 (2015).
33. U. Jena, N. Vaidyanathan, S. Chinnasamy and K. C. Das, *Bioresour. Technol.*, **102**(3), 3380 (2011).
34. G. Yu, Y. Zhang, L. Schideman, T. Funk and Z. Wang, *Energy Environ. Sci.*, **4**(11), 4587 (2011).
35. Y. H. Zhu, S. B. Jones, A. J. Schmidt, K. O. Albrecht, S. J. Edmundson and D. B. Anderson, *Algal Res.*, **39**, 101467 (2019).
36. Y. H. Zhang and L. Schideman, E^2-Energy, http://e2-energy.illinois.edu/ (Accessed March 6th 2011).
37. T. Selvaratnam, S. M. Henkanatte-Gedera, T. Muppaneni, N. Nirmalakhandan, S. Deng and P. J. Lammers, *Energy*, **104**, 16 (2016).
38. Y. Li, S. Leow, A. C. Fedders, B. K. Sharma, J. S. Guest and T. J. Strathmann, *Green Chem.*, **19**(4), 1163 (2017).
39. R. B. Madsen, P. Biller, M. M. Jensen, J. Becker, B. B. Iversen and M. Glasius, *Energy Fuels*, **30**(12), 10470 (2016).
40. R. Cherad, J. A. Onwudili, P. Biller, P. T. Williams and A. B. Ross, *Fuel*, **166**, 24 (2016).
41. C. Gai, Y. Zhang, W.-T. Chen, Y. Zhou, L. Schideman, P. Zhang, G. Tommaso, C.-T. Kuo and Y. Dong, *Bioresour. Technol.*, **184**, 328 (2015).
42. S. Edmundson, M. Huesemann, R. Kruk, T. Lemmon, J. Billing, A. Schmidt and D. Anderson, *Algal Res.*, **26**, 415 (2017).
43. D. C. Elliott, P. Biller, A. B. Ross, A. J. Schmidt and S. B. Jones, *Bioresour. Technol.*, **178**, 147 (2015).
44. J. L. Faeth, P. J. Valdez and P. E. Savage, *Energy Fuel*, **27**(3), 1391 (2013).
45. W. J. Liu, K. Tian, H. Jiang, X. S. Zhang, H. S. Ding and H. Q. Yu, *Environ. Sci. Technol.*, **46**(14), 7849 (2012).
46. J. F. Stanzione, P. A. Giangiulio, J. M. Sadler, J. J. La Scala and R. P. Wool, *ACS Sustain. Chem. Eng.*, **1**(4), 419 (2013).
47. P. Biller and A. B. Ross, *Bioresour. Technol.*, **102**(1), 215 (2011).
48. K. Anastasakis and A. B. Ross, *Bioresour. Technol.*, **102**(7), 4876 (2011).
49. D. R. Vardon, B. K. Sharma, J. Scott, G. Yu, Z. Wang, L. Schideman, Y. Zhang and T. J. Strathmann, *Bioresour. Technol.*, **102**(17), 8295 (2011).
50. P. J. Valdez, J. G. Dickinson and P. E. Savage, *Energy Fuel*, **25**(7), 3235 (2011).
51. Z. Srokol, A.-G. Bouche, A. van Estrik, R. C. J. Strik, T. Maschmeyer and J. A. Peters, *Carbohydr. Res.*, **339**(10), 1717 (2004).
52. W. T. Chen, Y. H. Zhang, J. X. Zhang, G. Yu, L. C. Schideman, P. Zhang and M. Minarick, *Bioresour. Technol.*, **152**, 130 (2014).
53. L. Qian, S. Wang and P. E. Savage, *Bioresour. Technol.*, **232**, 27 (2017).
54. W. T. Chen, Y. H. Zhang, J. X. Zhang, L. Schideman, G. Yu, P. Zhang and M. Minarick, *Appl. Energy*, **128**, 209 (2014).
55. P. T. Williams and J. Onwudili, *Ind. Eng. Chem. Res.*, **44**(23), 8739

(2005).
56. D. A. Nelson, P. M. Molton, J. A. Russell and R. T. Hallen, *Ind. Eng. Chem. Prod. Res. Dev.*, **23**(3), 471 (1984).
57. A. Sınağ, A. Kruse and V. Schwarzkopf, *Ind. Eng. Chem. Res.*, **42**(15), 3516 (2003).
58. G. C. A. Luijkx, F. van Rantwijk and H. van Bekkum, *Carbohydr. Res.*, **242**, 131 (1993).
59. P. Bohutskyi, M. J. Betenbaugh and E. J. Bouwer, *Bioresour. Technol.*, **155**, 366 (2014).
60. N. Sato, A. T. Quitain, K. Kang, H. Daimon and K. Fujie, *Ind. Eng. Chem. Res.*, **43**, 3217 (2004).
61. S. P. Zou, Y. L. Wu, M. D. Yang, K. Imdad, C. Li and J. M. Tong, *Energy*, **35**(12), 5406 (2010).
62. U. Jena and K. C. Das, *Energy Fuel*, **25**(11), 5472 (2011).
63. D. L. Barreiro, C. Zamalloa, N. Boon, W. Vyverman, F Ronsse, W. Brilman and W. Prins, *Bioresour. Technol.*, **146**, 463 (2013).
64. C. Torri, L. Garcia Alba, C. Samorì, D. Fabbri and D. W. F. Brilman, *Energy Fuel*, **26**(1), 658 (2012).
65. Y. F. Yang, C. P. Feng, Y. Inamori and T. Maekawa, *Resour. Conserv. Recycl.*, **43**(1), 21 (2004).
66. C. Y. Tian, Z. D. Liu, Y. H. Zhang, B. M. Li, W. Cao, H. F. Lu, N. Duan, L. Zhang and T. T. Zhang, *Bioresour. Technol.*, **184**, 336 (2015).
67. A. Sukenik, D. Tchernov, A. Kaplan, E. Huertas, L. M. Lubian and A. Livne, *J. Phycol.*, **33**, 969 (1997).
68. J. C. M. Carvalho, F. R. Francisco, K. A. Almeida, S. Sato and A. Converti, *J. Phycol.*, **40**, 589 (2004).
69. S. Belkin and S. Boussiba, *Plant Cell Physiol.*, **32**(7), 953 (1991).
70. C. Gai, Y. Zhang, W.-T. Chen, Y. Zhou, L. Schideman, P. Zhang, G. Tommaso, C.-T. Kuo and Y. Dong, *Bioresour. Technol.*, **184**, 328 (2015).
71. B. Maddi, E. Panisko, T. Wietsma, T. Lemmon, M. Swita, K. Albrecht and D. Howe, *Biomass Bioenergy*, **93**, 122 (2016).
72. I. Kulaev, V. Vagabov and T. Kulakovskaya, *J. Biosci. Bioeng.*, **88**(2), 111 (1999).
73. R. Shakya, S. Adhikari, R. Mahadevan, S. R. Shanmugam, H. Nam, E. B. Hassan and T. A. Dempster, *Bioresour. Technol.*, **243**, 1112 (2017).
74. L. Garcia Alba, C. Torri, C. Samorì, J. van der Spek, D. Fabbri, S. R. A. Kersten and D. W. F. Brilman, *Energy Fuel*, **26**(1), 642 (2011).
75. I. S. Chronakis, *J. Agr. Food Chem.*, **49**(2), 888 (2001).
76. A. A. Peterson, R. P. Lachance and J. W. Tester, *Ind. Eng. Chem. Res.*, **49**(5), 2107 (2010).
77. Y. Y. Wang and C. H. Wang, *J. Yantai Univ.* (In Chinese), **19**(2), 125 (2006).
78. J. G. Liu, J. P. Zhang, M. Y. Yin and Z. C. Meng, *Studia Marina Sinica* (In Chinese), **48**, 55 (2007).
79. X. F. Li, C. H. Wang and S. H. Wen, *Food Ferment Ind.* (In Chinese), **25**(4), 13 (1999).
80. S. L. Lou, L. G. Wu, C. X. He and Q. J. Wu, *J. Xiamen Univ.* (In Chinese), **35**(6), 955 (1996).
81. D. J. Shan and J. H. Gong, China Patent, ZL200910091011.4 (2009).
82. K. M. Wang, *J. Hangzhou Inst. Appl. Eng.* (In Chinese), **17**(3), 167 (2005).
83. T. Wu, Preliminary Study on the Influence of Nutrients on the Growth of Ulva prolifera and its Absorption of Different Nitrogen Species [Master Dissertation]. Qingdao China (2013).